Proceedings of The Institute of Acoustics

NEAR FIELD EFFECTS IN NON-LINEAR ACOUSTICS

B.V.Smith*, H.O.Berktay†, B.S.Cooper**, J.R.Dunn*
*University of Birmingham, †University of Bath, formerly University of Birmingham.
** Formerly University of Birmingham

INTRODUCTION

The aim of this paper is to present a sample of experimental results obtained from some investigations into the near-field behaviour of finite-amplitude waves and to compare this data with existing theoretical models.

Two aspects of this non-linear behaviour are examined; extra-attenuation effects and the Parametric array.

EXTRA-ATTENUATION

Theoretical considerations

As a finite-amplitude wave propagates underwater, energy is lost from the fundamental frequency component through non-linear interactions. Extra-attenuation is a measure of the reduction in the amplitude of the fundamental and is defined, as for example in reference 1, as the attenuation which is in excess of that predicted by geometrical spreading and small-signal absorption.

Studies have been made on the extra-attenuation in finite-amplitude planar waves[1], spherically spreading waves[2] and cylindrically spreading waves[3]. The extra-attenuation in waves transmitted from planar pistons with square or circular apertures has also been examined[3,4], by using propagation models in which the axial field of the piston is considered to be split into a planar collimated near-field zone, where most of the extra-attenuation occurs, and a far-field spherically spreading zone. The investigations reported here are concerned with the extra-attenuation in waves transmitted from rectangular planar apertures of differing aspect ratios, N, greater than unity.

Now it has been established[5] that waves with planar, spherical and cylindrical geometries which are propagating in lossless media may be described by a single wave equation in which a 'stretching function' is used for the range normalized to the shock distance. This has the effect of making the non-linear behaviour appear the same for all three basic wave types. It is also known[1] that a finite-amplitude wave, which has a large acoustic Reynold's number, Γ, as defined in reference 1, and is propagating in a medium with absorption, behaves almost identically to a wave in a lossless medium. Using these ideas the present authors[3] were able to predict extra-attenuation curves for waves with spherical and cylindrical geometries from the planar wave data contained in reference 1. Use was also made of the criteria that the 'old-age' region is reached when the shock width, Δ, as defined in reference 1, is of the order of $1.2/\pi$.

Consequently, it is tempting to speculate further that finite-amplitude waves of large Γ and with more complex propagation geometries, have extra-attenuation characteristics predicted by the plane wave curve, also for large Γ, shown in Fig.1. Providing, in addition, that the appropriate stretching function, σ_{EFF}, is used in place of σ. For plane waves $\sigma_{EFF} = \sigma$ and is the normalized range R/L, where L is the shock distance, which is given by $L = (\beta\epsilon k)^{-1}$, where β is a non-linear parameter (of the order of 3.5 for water) k is the wavenumber and ϵ is the acoustic Mach number. The Mach number is defined as the ratio of the peak particle velocity, $\hat{u}$, at the source boundary, to the small-amplitude sound speed, C_o.

The stretching function, σ_{EFF} may be defined:-

$$\sigma_{EFF} = \frac{\beta}{C_o} \int_{R_o}^{R} \frac{\partial u}{\partial r}\Big|_o dr \quad ,$$

where $\frac{\partial u}{\partial r}\Big|_o$, is the differential of the particle velocity with respect to range evaluated at a zero crossing of the velocity waveform, R is the observation range and R_o is the position of the source boundary. It follows that for plane waves, $R_o = 0$ and $\sigma_{EFF} = R\,\beta\epsilon k = R/L = \sigma$, for spherically spreading waves, R_o = the source radius and

$$\sigma_{EFF} = \sigma_o\, \ell n\left(\frac{\sigma}{\sigma_o}\right), \text{ where } \sigma_o = R_o/L,$$

for cylindrically spreading waves, R_o = the source radius and $\sigma_o = R_o/L$.

then $\sigma_{EFF} = 2\sqrt{\sigma_o}\,(\sqrt{\sigma} - \sqrt{\sigma_o})$. The stretching function for other geometries may also be derived. For example, if it is assumed that the radiation from a planar rectangular piston of size 2b x 2b/N(where, N, is the aspect ratio and is greater than unity), has a particle velocity amplitude, $|U|$, with a dependence on axial range of the form:-

$$|U|/\hat{U} = \left[1 + \left(\frac{R}{R_{o1}}\right)\right]^{-\frac{1}{2}}, \text{ where } R_{o1} = 4\left(\frac{b}{N}\right)^2/\lambda, \text{ then } \sigma_{EFF} \text{ becomes}$$

$$2\sigma_o\left[\left(1 + \frac{\sigma}{\sigma_o}\right)^{\frac{1}{2}} - 1\right], \quad \ldots\ldots\ldots\ldots\ldots\ldots\ldots\ldots\ldots\ldots\ldots(1)$$

where $\sigma_o = R_{o1}/L$.

Experimental Considerations

A rectangular transducer was constructed from four 7.6 cm square ceramic plates, whose thickness resonances were in the region of 300 kHz. The aspect ratio could therefore be varied from 1 to 4 by driving different combinations of plates. In addition, by adding masks, values of 6 and 8 for the aspect ratio could also be obtained.

Extra-attenuation measurements were made as a function of axial range and acoustic intensity. Empirical values of σ_{EFF} were then read off the weak shock curve of Fig.1 corresponding to the measured values of extra-attenuation. Now, for a fixed range, all the theoretical expressions for σ_{EFF} given in the previous section, predict that σ_{EFF} is proportional to the Mach number, ϵ, i.e. for a particular transducer, it is proportional to $(W)^{\frac{1}{2}}$, where W is the acoustic power. Therefore, graphs were plotted of the empirical values of σ_{EFF} against $(W)^{\frac{1}{2}}$ for each range. The results for the N=2 case, for example, are shown in Fig.2 and the results obtained at other aspect ratios are similar. The graphs, for each range, show good agreement for the predicted linear dependence of σ_{EFF} on $(W)^{\frac{1}{2}}$.

NEAR-FIELD EFFECTS IN NON-LINEAR ACOUSTICS

Graphs were also plotted of the empirical value of σ_{EFF} against the normalized range parameter, $\sigma = R/L$, for different intensities. Some examples of these graphs are shown in Figs. 3 and 4 for N=2 and N=4 respectively. If extra-attenuation were exactly predicted by plane wave theory then these graphs would follow the $\sigma_{EFF} = \sigma$ curves which are plotted as dashed curves in Figs. 3 and 4. For ranges less than about 3m the values of σ_{EFF} may be seen to follow the plane wave curve in shape but lie above the curve $\sigma_{EFF} = \sigma$, i.e. $\sigma_{EFF} > \sigma$. This indicates that the extra-attenuation measured at these ranges was greater than predicted by plane-wave theory. This trend was observed for all measurements made and is probably a consequence of the non-uniform axial pressure-amplitude distribution in the 'collimated' region of the near-field. Beyond the 3m range the experimental results generally fall below the $\sigma_{EFF} = \sigma$ curve, ie. $\sigma_{EFF} < \sigma$, and the extra attenuation at these ranges is therefore less than is predicted by plane-wave theory. The dotted curves on Figs. 3 and 4 are for the theoretical expression for σ_{EFF}, given by (1) above, for a range of 7m. From Fig.3, for N=2, it may be seen that this curve gives a good prediction of extra-attenuation at 7m. As the range increases, for any particular acoustic intensity, it may be observed from Fig.3, that the extra-attenuation characteristics change gradually from a plane-wave model to a model incorporating a spreading component as one might expect.

For the case N=4, Fig.4, there is a very interesting feature. In the region 2 to 3m there is a reduction in σ_{EFF} and this corresponds to a reduction in extra-attenuation. Also, in this region the curves apparently change over quite sharply from the dashed curve of the plane-wave model to the dotted curve of the plane-cylindrically spreading wave model. It is believed that this is again a consequence of the non-uniform axial pressure amplitude and phase structure associated with the near field but further theoretical and experimental investigations are needed to clarify this.

Beyond the 'old-age' range the curves of Figs. 3 and 4 would be expected to 'saturate', ie. σ_{EFF} would become constant independent of σ. In fig. 4 it may be noted that the final points on each intensity curve, which correspond to a range of 7m, are begining to deviate from the predicted curves. This is possibly an indication that the 'old-age' region is being approached. A curve drawn, such as to pass through the knee of this saturation characteristic would then provide information on the effective value of σ_o to be used to give the extra-attenuation to be expected in the far-field for this particular case. The 'old-age' region, as already indicated above is defined by the shock width equalling $1.2/\pi$, but how this is incorporated into the plane-cylindrical model discussed above remains to be determined. One further complication arises in relation to the position of the start of the 'old-age' region in relation to the distance $R_{O2} = 4b^2/\lambda$. Beyond this distance the axial distribution approaches a spherically spreading law and hence if the 'old-age' region occurs beyond R_{O2}, then the plane cylindrical model would need to be adapted.

An example of the effect of extra-attenuation on the directivity pattern measured at 30.2m for the N=4 transducer in the wide beam direction is shown in Fig. 5. The reduction in the ratio of the main lobe amplitude to the sidelobe level, because of extra-attenuation, is clearly visible for the high intensity pattern as compared to the pattern measured at a low intensity.

NEAR-FIELD EFFECTS IN NON-LINEAR ACOUSTICS

PARAMETRIC ARRAY

A considerable amount of information on the far-field behaviour of parametric arrays has been published both for absorption limited and saturation limited conditions. The references are too numerous to include here but reference 6 contains a comprehensive list. Some theoretical results have also been published on the near-field behaviour for the absorption limited case, eg. references 7 and 8. There is however very little information on the near-field behaviour when the array is saturation limited. Also, when the array is saturation limited there are still some anomalies between measurement and theory for the far-field of the parametric array[6].

A circular transducer of 15cm nominal diamter was driven at two frequencies centered on 324.5 kHz, with a difference frequency which was varied in the range 3 to 30 kHz. Some axial difference-frequency pressure amplitude measurements were made at difference frequencies of 3, 6 and 10 kHz and Fig.6 shows a typical set of data taken at low intensities. For these measurements the acoustic intensity at the source surface for each primary frequency wave was 0.063 Watts/cm^2 and at this level the parametric array was being operated in an absorption-limited mode. The two asymptotes shown on each difference frequency curve in Fig.6 are theoretical estimates based upon the near-field theory of reference 7 and the far-field interaction zone theory of reference 8. The agreement between theory and experiment is quite reasonable.

Corresponding experiments at higher levels of intensities equal to 2.53 W/cm^2 per primary wave, are shown in Fig.7 and under these circumstances the parametric array was being operated in a saturation-limited mode. The far-field asymptotes shown are calculated from the theoretical saturation limited model of reference 9. In this model the taper function used to describe the extra-attenuation of the primary waves ignores the additional attenuation introduced by the non-linear interaction between the primaries. An improved theoretical model which takes account of these additional interaction losses is proposed in reference 6 but this gives a figure for the difference-frequency sound pressure level (S.P.L) 5.4 dB lower than the asymptotes plotted in Fig.7. Thus better agreement is given by the theoretical model which ignores the interactive losses in describing the primary wave taper functions. In Fig. 8, experimental data points for the difference-frequency S.P.L are plotted against 'downshift ratio', f_o/f_- , where f_o and f_- are the mean primary frequency and difference frequency respectively. The range was 5m and the acoustic intensity was 2.53 W/cm^2 per primary wave. The two theoretical lines are estimates based upon the two models of reference 6 and 9 which have been discussed above. A similar graph was presented in reference 6 where the experimental data suggested a frequency dependence for the S.P.L of the form $-34 \log(f_o/f_-)$. The data in Fig.8 suggests a frequency dependence very similar to this.

In some earlier unpublished work[10] a crude taper function was used to describe the extra-attenuation of the primary waves so as to enable theoretical predictions to be made of the dependence of the 3dB beamwidth (at the difference frequency) on the acoustic intensity in the primary waves. The conclusions reached in reference 10 were that the beamwidth spreading was more accurately predicted by using a taper function which ignored additional interactive losses because of the presence of both primary waves. The downshift ratios used in reference 10 were 18.6 and 10.3. Thus these conclusions are broadly in agreement with the results quoted in reference 6 and the results reported here.

The reason for this anomaly was attributed in reference 10, to the transfer of energy to the difference-frequency wave from higher order non-linear interactions between the primary waves and their harmonics. For example, some of the additional energy which is lost from the primary waves because of the interactions between one primary and another would be returned to the difference-frequency wave because of interactions of harmonics such as $2f_1-f_2$ and $2f_2-f_1$ with f_1 and f_2 respectively, where f_1 and f_2 are the respective primary wave frequencies. The detailed contribution of these additonal sources of difference-frequency energy to the overall signal will of course depend upon the relative phases.

Fig.9 shows two 10kHz difference-frequency beam patterns taken with this circular source at low and high intensities respectively measured at a range of 6m. The beam broadening is apparent.

For the rectangular array with N=4 some beam patterns, measured at 30.2m at difference frequencies of 10kHz and 20kHz are plotted in Fig.10. The effect of the source aperture[6] on the sharpening of the skirts of the 20kHz beam as compared to the 10kHz beam may be clearly seen.

ACKNOWLEDGEMENTS

The authors aknowledge the support of the Procurement Executive of the Ministry of Defence.

REFERENCES

1. D.T.Blackstock, 1964, "Thermoviscous attenuation of plane, periodic, finite-amplitude sound waves". J.Acoust.Soc.Am. 36, No3, 534-542.

2. B.B.Carey, 1967, "Nonlinear losses induced in spherical waves". J.Acoust. Soc.Am. 42, No.1, 88-92.

3. H.O.Berktay and B.V.Smith, 1968, "Finite-amplitude effects in transmitting devices exploiting non-linearities in acoustic propagation", paper read at British Acoust. Soc. meeting, Weymouth (unpublished).

4. H.M.Merklinger, 1971, "High intensity effects in the non-linear acoustic parametric end-fire array". Ph.D. thesis (unpublished), University of Birmingham.

5. D.T.Blackstock, 1964, "On plane, spherical and cylindrical sound waves of finite amplitude in lossless fluids." J.Acoust.Soc.Am. 36, No.1, 217-219.

6. M.B.Moffett and R.H.Mellen, 1977, "Model for parametric acoustic sources". J.Acoust.Soc.Am. 61, No.2, 325-337.

7. H.O.Berktay, 1971, "Near-field effects in parametric end-fire arrays". University of Birmingham, Department of Electronic and Electrical Engineering Memorandum No.418.

8. R.L.Rolleigh, 1975, "Difference frequency pressure within the interaction region of a parametric array". J.Acoust.Soc.Am., 58, No.5, 964-971.

9. J.F.Bartram, 1972, "A useful analytical model for the parametric acoustic array". J.Acoust.Soc.Am., 52, No.3, 1042-1044.

10. B.V.Smith, 1967, "Nonlinear acoustics with emphasis on transmitting applications" Ph.D. thesis (unpublished) University of Birmingham.

Fig.1

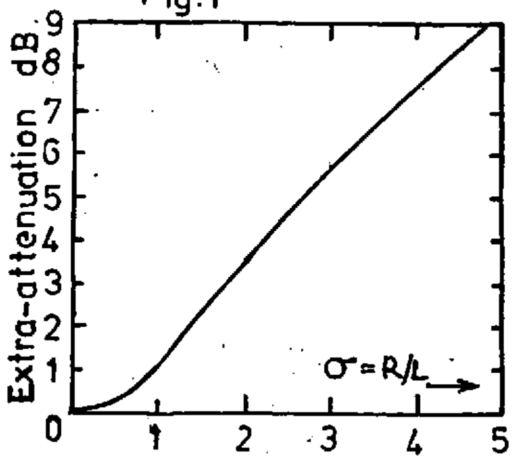

Fig. 2 N = 2

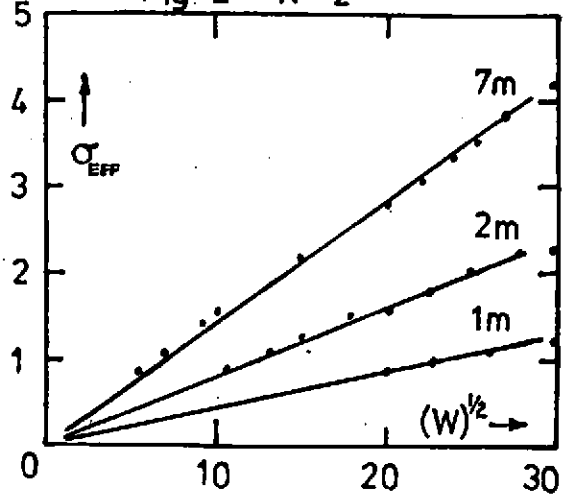

Fig.3 N = 2

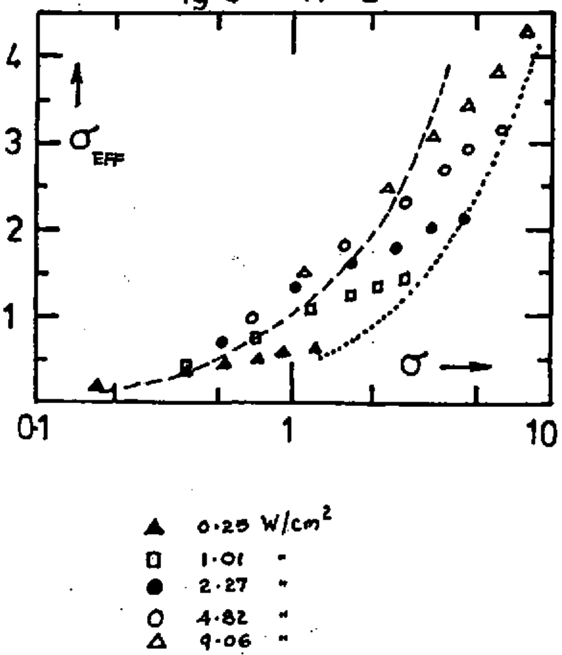

Fig. 4 N = 4

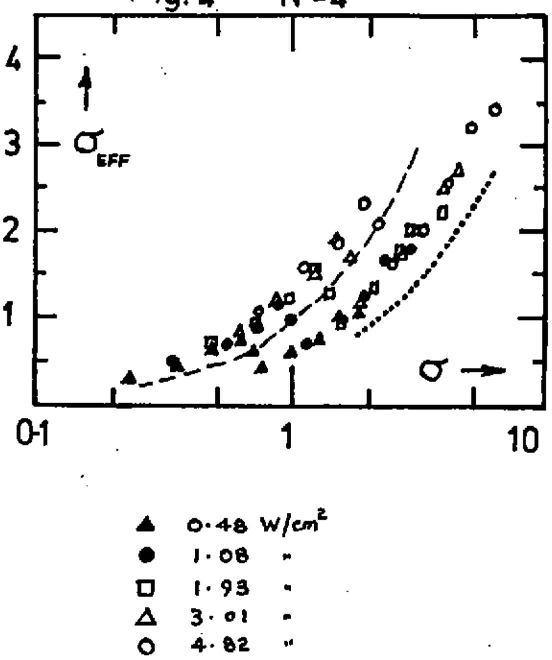

Fig. 5

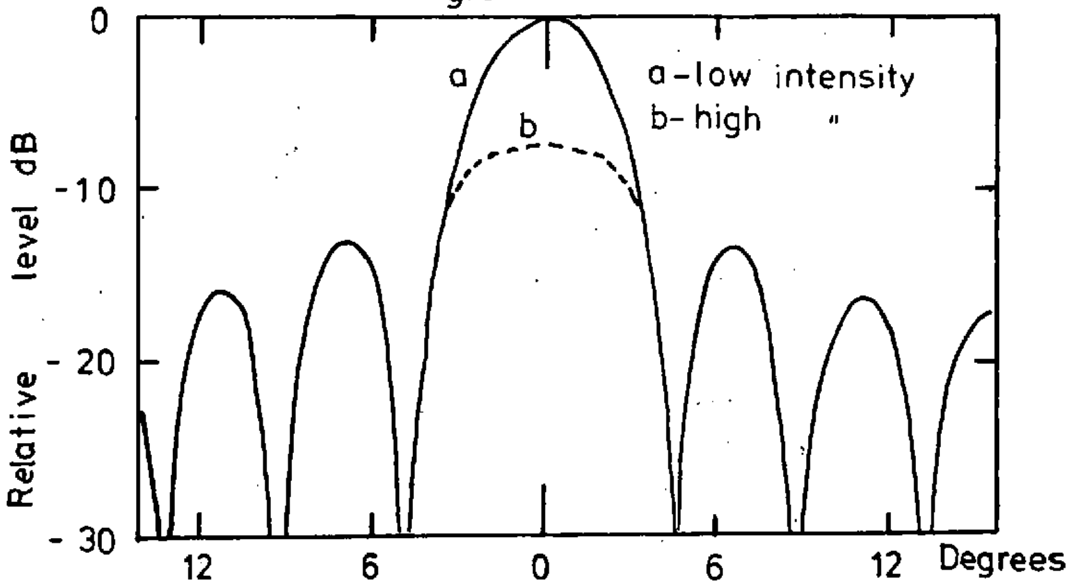

Fig. 6

0·063 W/cm²

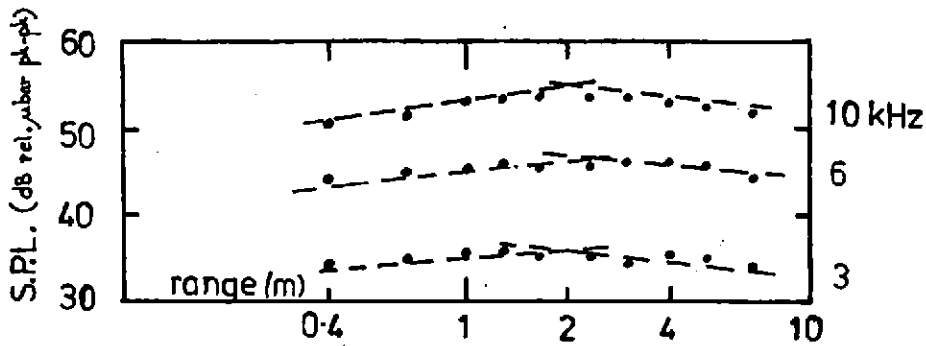

Fig. 7

2·53 W/cm²

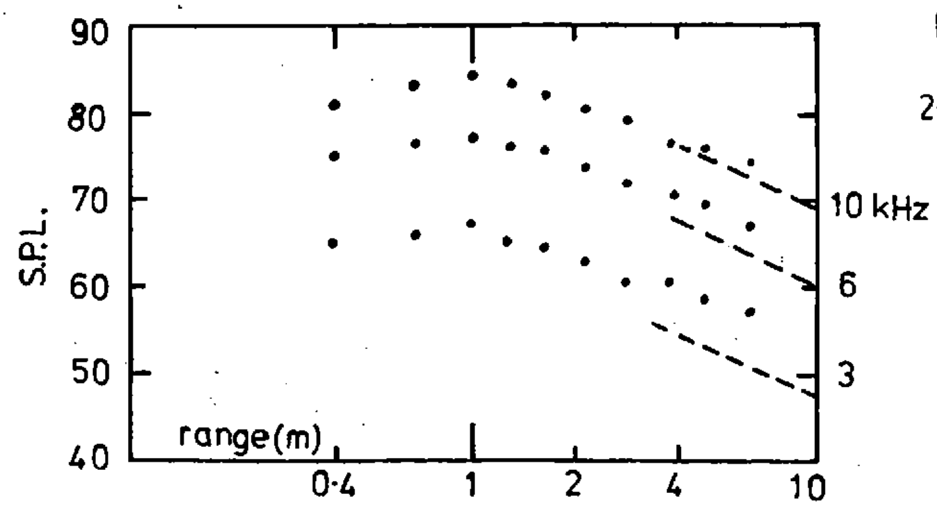

Fig. 8

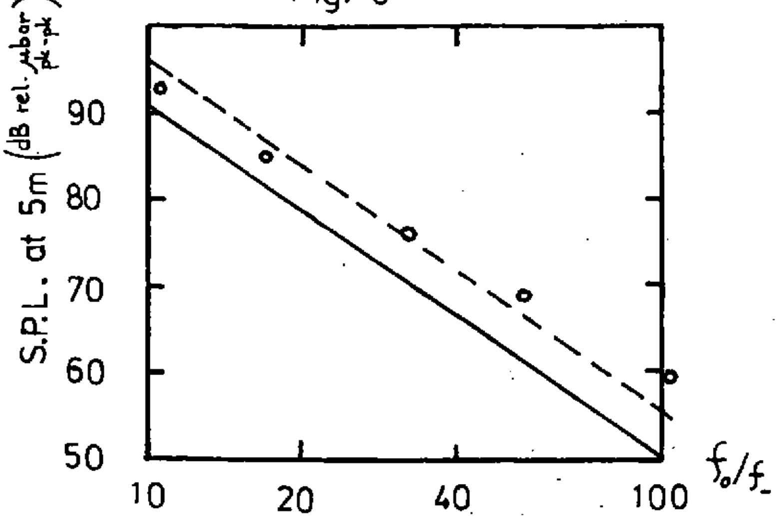

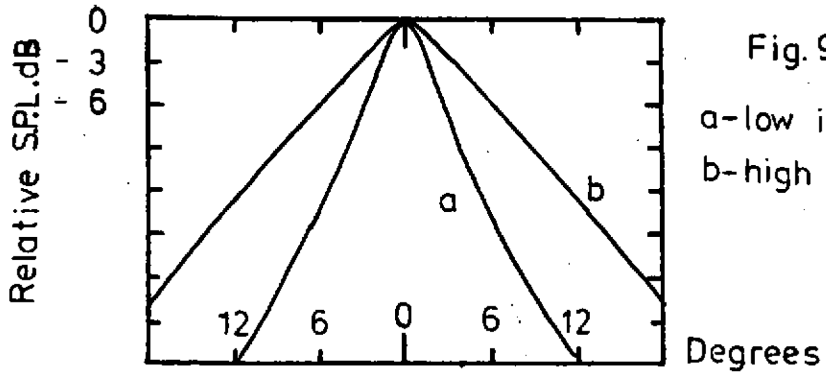

Fig. 9

a-low intensity
b-high "

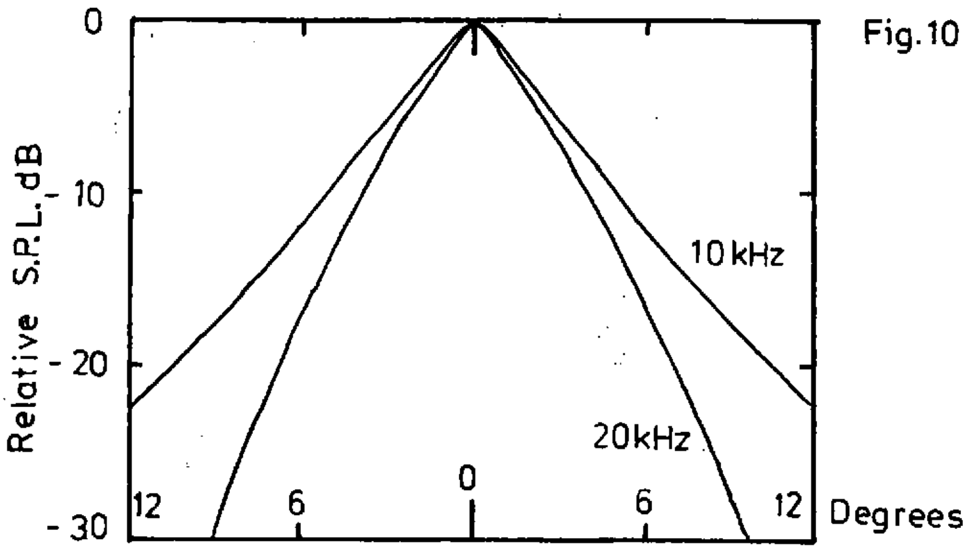

Fig. 10